Test of trajectory calculations against quantum mechanical state-to-state and thermal collinear reaction rates for H + Cl2 → HCl + Cl

ARTICLE *in* THE JOURNAL OF PHYSICAL CHEMISTRY · APRIL 1979

Impact Factor: 2.78 · DOI: 10.1021/j100471a030

3 AUTHORS, INCLUDING:

Donald Truhlar
University of Minnesota Twin Cities
1,342 PUBLICATIONS **82,669** CITATIONS
SEE PROFILE

Michael Baer
Hebrew University of Jerusalem
345 PUBLICATIONS **8,264** CITATIONS
SEE PROFILE

(8) R. A. LaBudde, P. J. Kuntz, R. B. Bernstein, and R. D. Levine, *Chem. Phys. Lett.*, **19**, 7 (1973); *J. Chem. Phys.*, **59**, 6286 (1973).
(9) (a) A. M. Rulis and R. B. Bernstein, *J. Chem. Phys.*, **57**, 5497 (1972); (b) R. B. Bernstein and A. M. Rulis, *Faraday Discuss., Chem. Soc.*, **55**, 293 (1973).
(10) W. E. Wentworth, R. George, and H. Keith, *J. Chem. Phys.*, **51**, 1791 (1969).
(11) The empirical function is essentially a Morse potential with the following modifications: (i) multiplying the attractive term by an adjustable parameter k, which is a function of the dissociation energy of CH_3–X (D_{0,CH_3-X}) and the electron affinity of the halogen atom (EA_X), (ii) subtracting the EA_X from the potential resulting from (i).
(12) G. Herzberg, "Molecular Spectra and Molecular Structure", Vol. III, "Electronic Spectra and Electronic Structure of Polyatomic Molecules", Van Nostrand, Princeton, N.J., 1966.
(13) D. R. Stull and H. Prophet, *Natl. Stand. Ref. Data Ser., Natl. Bur. Stand.*, **No. 37** (1970).
(14) B. deB Darwent, *Natl. Stand. Ref. Data Ser., Natl. Bur. Stand.*, **No. 31** (1970).
(15) R. S. Berry and C. W. Reinmann, *J. Chem. Phys.*, **38**, 1540 (1963).
(16) If the bottom of the CH_3X potential well were taken as the initial state, the addition of the zero-point vibrational energy of CH_3X to E_b will produce a larger difference in threshold upon comparing theory and experiment (see Table II).
(17) (a) K. T. Wu, H. F. Pang, and R. B. Bernstein, unpublished results. (b) Because of experimental difficulties, the high translational thresholds for the CH_3Cl and CH_3F systems could not be determined.
(18) J. A. Kerr, E. A. Lissi, and A. F. Trotman-Dickenson, *J. Chem. Soc.*, 1673 (1964).
(19) J. C. Polanyi, *Acc. Chem. Res.*, **5**, 161 (1972).
(20) G. G. Balint-Kurti, *Mol. Phys.*, **25**, 393 (1973).
(21) C. W. A. Evers and A. E. de Vries, *Chem. Phys.*, **15**, 201 (1976).
(22) Equilibrium distance of r_{C-X} is assigned to be the lower limit.
(23) J. A. Aten and J. Los, *Chem. Phys.*, **25**, 47 (1977).
(24) J. A. Aten, C. W. A. Evers, A. E. de Vries, and J. Los, *Chem. Phys.*, **23**, 125 (1977).
(25) (a) A. P. M. Baede, *Physica*, **59**, 541 (1972); (b) A. P. M. Baede, D. J. Auerbach, and J. Los, *ibid.*, **64**, 134 (1973); (c) D. J. Auerbach, M. M. Hubers, A. P. M. Baede, and J. Los, *Chem. Phys.*, **2**, 107 (1973).
(26) M. M. Hubers, A. W. Kleyn, and J. Los, *Chem. Phys.*, **17**, 303 (1976).

Test of Trajectory Calculations against Quantum Mechanical State-to-State and Thermal Collinear Reaction Rates for H + Cl_2 → HCl + Cl

Joni C. Gray, Donald G. Truhlar,*

Chemical Dynamics Laboratory, Kolthoff and Smith Halls, Department of Chemistry, University of Minnesota, Minneapolis, Minnesota 55455

and Michael Baer

Soreq Nuclear Research Center, Yavne, Israel, and Department of Chemical Physics, The Weizmann Institute of Science, Rehovot, Israel *(Received August 31, 1978)*

State-to-state, state-selected, and completely thermal rate constants and associated Arrhenius parameters are computed for the collinear H + Cl_2 reaction using new quantum mechanical reaction probabilities. Thermal rate constants for production of specific final states and the mean fraction of available energy in vibrational excitation energy of the product are also computed. These results are compared systematically to previous trajectory calculations of the same quantitites. Three different trajectory methods are considered.

I. Introduction

In previous studies, extensive trajectory calculations were carried out for the collinear exothermic reaction H + Cl_2 → HCl + Cl.[1,2] In the first study, the trajectories were used to calculate state-to-state and total reaction probabilities using the standard quasiclassical trajectory method[3] with histogram assignment[4,5] of final states, using the quasiclassical trajectory reverse histogram method,[6,7] and using the Bessel uniform approximation[8-10] of classical S matrix theory. From these probabilities the state-to-state and thermal reaction rate constants were calculated by integration, and the associated Arrhenius parameters were calculated by fitting the rates over various temperature ranges. For comparison the corresponding rate constants and Arrhenius parameters were calculated from the most accurate quantum mechanical state-to-state and total reaction probabilities then available[11] for the same system. The study included three vibrational states of the reactants and up to seven vibrational states of the products and is the most systematic and complete comparison of quasiclassical and quantal computations of reaction rates available. Subsequently, accurate quantal state-to-state and total reaction probabilities were obtained for this system, and they have been used for two less extensive tests of quasiclassical trajectory calculations.[2,12] One of these contained a comparison between the H + Cl_2 and D + Cl_2 reactions, and the other contained a study of the temperature dependence of the activation energy. In the present study we integrate the more accurate quantal reaction probabilities to compute a complete set of state-to-state and thermal reaction rates and associated Arrhenius parameters for comparison with the trajectory calculations of ref 1. To make the comparisons more definitive, we also carried out a few additional high-energy trajectory calculations; and to make the comparisons more consistent, we used the same computational schemes as used for the quantal results to recalculate state-to-state and thermal reaction rates and associated Arrhenius parameters from the reaction probabilities obtained from the trajectory calculations.

Other comparisons of quantal and quasiclassical state-to-state reaction rates and Arrhenius parameters in the literature are for collinear H + H_2,[13] collinear F + H_2[14] and F + D_2,[15] and collinear H_2 + I.[16] Other comparisons of quantal and quasiclassical thermal rate constants and Arrhenius parameters in the literature are for three-dimensional H + H_2,[3,17] collinear H + H_2,[13] collinear Cl + H_2 and isotopic analogues,[18] and collinear H_2 + I.[16] These comparisons of thermal rate constants have recently been reviewed.[19]

0022-3654/79/2083-1045$01.00/0

II. Calculations

A. Potential Energy Surface. The potential energy surface for the system considered here is the one used by Kuntz et al.[20] and one of the authors.[11] The classical barrier height is 2.42 kcal/mol.[1]

B. Vibrational Energies. The vibrational energies are given in Table I of ref 1.

C. Trajectories. The additional trajectory calculations were carried out using the methods described in ref 1.

D. Rate Constants. State-to-state rate constants were calculated from

$$k_{n_1n_2}(T) = (2\pi\mu kT)^{-1/2}\int_{E_{\text{lower}}}^{\infty} P^{\text{R}}_{n_1n_2}(E_{\text{rel}})e^{-E_{\text{rel}}/kT}\,\mathrm{d}E_{\text{rel}} \quad (1)$$

where T is the temperature, μ and E_{rel} are the reduced mass and translational energy for relative motion, and $P^{\text{R}}_{n_1n_2}(E_{\text{rel}})$ is the state-to-state reaction probability for initial vibrational quantum number n_1 and final vibrational quantum number n_2. State-selected rate constants were calculated from

$$k_{n_1}(T) = (2\pi\mu kT)^{-1/2}\int_{E_{\text{lower}}}^{\infty} P^{\text{R}}_{n_1}(E_{\text{rel}})e^{-E_{\text{rel}}/kT}\,\mathrm{d}E_{\text{rel}} \quad (2)$$

where

$$P^{\text{R}}_{n_1}(E_{\text{rel}}) = \sum_{n_2=0}^{7} P^{\text{R}}_{n_1n_2}(E_{\text{rel}}) \quad (3)$$

The quadratures (1) and (2) were carried out by the trapezoidal rule with step size 0.03 kcal/mol. The probabilities were obtained at the quadrature abscissas by a quadratic interpolation of the probabilities, except when the quadratically interpolated value did not satisfy $0 \le P^{\text{R}} \le 1$. The total energy is defined by

$$E = E_{\text{rel}} + E^{\text{v}}_{n_1} \quad (4)$$

where $E^{\text{v}}_{n_1}$ is the initial vibrational energy.

The new quantum mechanical reaction probabilities are available for E = 2.307–11.534 kcal/mol for $n_1 = 0$, E = 3.691–11.534 kcal/mol for $n_1 = 1$, and E = 4.613–11.534 kcal/mol for $n_1 = 2$. The available probabilities were extrapolated exponentially to $E_{\text{rel}} = 0$ for each n_1. For energies $E \ge 13$ kcal/mol the quantum mechanical reaction probabilities required for (1) were approximated by the quasiclassical trajectory histogram ones. Possible errors for the quantum mechanical $k_{n_1n_2}(T)$ and $k_{n_1}(T)$ due to interpolation and extrapolation were obtained by comparing the best estimate to values obtained by three other methods of interpolation with the same extrapolation and all four methods of interpolation with low-energy linear extrapolation of the probability to $P^{\text{R}} = 0$. The error estimate is the largest of the seven deviations.

Rate constants were calculated from the trajectory calculations using the same techniques except interpolation of the probability is used instead of extrapolation near threshold and the classical S matrix probabilities are approximated as constants at high energies that contribute almost negligibly. Possible interpolation errors were estimated as the largest deviation of three other methods of interpolation from the best estimate.

Rate constants for production of a specific final state were calculated as

$$k^{n_2}(n_1{\le}2;T) = \sum_{n_1=0}^{2} P_{n_1}(T)k_{n_1n_2}(T) \quad (5)$$

where the probability that the initial vibrational state is n_1 at temperature T is

$$P_{n_1}(T) = \frac{\exp(-E^{\text{v}}_{n_1}/kT)}{Q^{\text{v}}(T)} \quad (6)$$

and the vibrational partition function is

$$Q^{\text{v}}(T) = \sum_{n_1} \exp(-E^{\text{v}}_{n_1}/kT) \quad (7)$$

The vibrational partition function was converged (summed through $n_1 = 14$). Note that states with $n_1 \ge 2$ do not always make completely negligible contributions to the rate constants for production of a specific final state, but they are systematically excluded from eq 5 because of insufficient data.

Two different values were calculated for the thermal rate constant $k(T)$. The first is the contribution of initial states n_1 = 0–2:

$$k(n_1{\le}2;T) = \sum_{n_1=0}^{2} P_{n_1}(T)k_{n_1}(T) \quad (8)$$

The second involves a simple estimate of the contribution of higher initial states:

$$k(T) = \sum_{n_1=0}^{1} P_{n_1}(T)k_{n_1}(T) + [1 - P_0(T) - P_1(T)]k_2(T) \quad (9)$$

E. Arrhenius Parameters. The Arrhenius activation energies $E_a(n_1,n_2,T)$ and $E_a(n_1,T)$ for state-to-state rate constants $k_{n_1n_2}(T)$ and state-selected rate constants $k_{n_1}(T)$ were calculated by the Tolman method as[12]

$$E_a(n_1,n_2,T) = \frac{(2\pi\mu kT)^{-1/2}\int_{E_{\text{lower}}}^{\infty} E_{\text{rel}}P^{\text{R}}_{n_1n_2}(E_{\text{rel}})e^{-E_{\text{rel}}/kT}\,\mathrm{d}E_{\text{rel}}}{k_{n_1n_2}(T)} - \tfrac{1}{2}kT \quad (10)$$

and

$$E_a(n_1,T) = \frac{(2\pi\mu kT)^{-1/2}\int_{E_{\text{lower}}}^{\infty} E_{\text{rel}}P^{\text{R}}_{n_1}(E_{\text{rel}})e^{-E_{\text{rel}}/kT}\,\mathrm{d}E_{\text{rel}}}{k_{n_1}(T)} - \tfrac{1}{2}kT \quad (11)$$

using the same techniques as for integrating the rate constants. The preexponential factors $A(n_1,n_2,T)$ and $A(n_1,T)$ at temperature T were then calculated by solving

$$k_{n_1n_2}(T) = A(n_1,n_2,T)\exp[-E_a(n_1,n_2,T)/kT] \quad (12)$$

and

$$k_{n_1}(T) = A(n_1,T)\exp[-E_a(n_1,T)/kT] \quad (13)$$

Arrhenius activation energies for $E_a(T)$ for the thermal rate constants $k(T)$ were also calculated by the Tolman method.[21] According to this method, for a collinear reaction

$$E_a(T) = E^{\text{rel}}_a(T) + E^{\text{v}}_a(T) \quad (14)$$

$$E^{\text{rel}}_a(T) = \langle E_{\text{rel}}\rangle^{\text{T}}_{\text{reactions}} - \tfrac{1}{2}kT \quad (15)$$

$$\langle E_{\text{rel}}\rangle^{\text{T}}_{\text{reactions}} = \frac{\sum_{n_1}P_{n_1}(T)\int_{E_{\text{lower}}}^{\infty} E_{\text{rel}}P^{\text{R}}_{n_1}(E_{\text{rel}})\exp(-E_{\text{rel}}/kT)\,\mathrm{d}E_{\text{rel}}}{(2\pi\mu kT)^{1/2}k(T)} \quad (16)$$

$$E^{\text{v}}_a(T) = \langle E^{\text{v}}_{n_1}\rangle^{T}_{\text{reactions}} - \langle E^{\text{v}}_{n_1}\rangle^{T} \quad (17)$$

$$\langle E^{v}_{n_1}\rangle^{T}_{\text{reactions}} = \frac{\sum_{n_1} E^{v}_{n_1} P_{n_1}(T) \int_{E_{\text{lower}}}^{\infty} P^{R}_{n_1}(E_{\text{rel}}) \exp(-E_{\text{rel}}/kT)\, dE_{\text{rel}}}{(2\pi\mu kT)^{1/2} k(T)} \quad (18)$$

$$\langle E^{v}_{n_1}\rangle T = \frac{\sum_{n_1} E^{v}_{n_1} \exp(-E^{v}_{n_1}/kT)}{Q^{v}(T)} \quad (19)$$

The calculation of $k(T)$, $Q^{v}(T)$, and the integral in eq 18 has already been discussed. The numerators of eq 16, 18, and 19 were summed to convergence; for (16) and (18) this required assumptions about $P_{n_1}(E_{\text{rel}})$ for $n_1 > 2$. Since these higher vibrational states make only small contributions we used the simple estimate that $P_{n_1}(E_{\text{rel}})$ equals $c(T)$ for $n_1 > 2$ where $c(T)$ is a constant for each integration but depends parametrically on temperature. At each temperature we choose $c(T)$ equal to $\langle P^{R}_{2}\rangle^{T}$ where

$$\langle P^{R}_{2}\rangle^{T} = \frac{k_2(T)}{(2\pi\mu kT)^{-1/2} \int_0^{\infty} \exp(-E_{\text{rel}}/kT)\, dE_{\text{rel}}} \quad (20)$$

F. Fraction of Final Energy in Vibration. The trajectory calculations of these quantities were not repeated. For the quantum mechanical results we used the following procedure. The state-selected fraction $f_{n_1}(E)$ of available excitation energy E^{ae} (defined as total energy in excess of product zero-point energy) which is released as vibrational excitation energy of the product was computed as a function of total energy E above the bottom of the reactant potential well by eq 12 and 13 of ref 1. The average fraction $f_{n_1}(T)$ of available excitation energy which appears as product vibrational excitation for initial-state-selected reactions with initial vibrational quantum number n_1 and translational temperature T was computed from

$$f_{n_1}(T) = \frac{\sum_{n_2} f^{ae}[n_2, E^{ae}_{n_1}(T)] k_{n_1 n_2}(T)}{k_{n_1}(T)} \quad (21)$$

where

$$f^{ae}(n_2, E^{ae}) = \frac{E^{v}_{n_2}(\text{product}) - E^{v}_{0}(\text{product})}{E^{ae}} \quad (22)$$

and the denominator of eq 22 was taken for approximate consistency with ref 1 as

$$E^{ae}_{n_1}(T) = \Delta E + kT + E_a(n_1, T) - E^{v}(\text{product}) \quad (23)$$

where ΔE is the classical exoergicity and $E_a(n_1, T)$ was computed as discussed in subsection E above. The average fraction $f(T)$ of available excitation energy which appears as product vibrational excitation energy in a thermal system was calculated from

$$f(T) = \frac{\sum_{n_2} f^{ae}[n_2, E^{ae}(T)] k^{n_2}(T)}{k(T)} \quad (24)$$

where the denominator of eq 22 was taken for approximate consistency with ref 1 as

$$E^{ae}(T) = \Delta E + kT + E_a(T) - E^{v}_{0}(\text{product}) \quad (25)$$

in terms of the Tolman activation energy $E_a(T)$ of subsection E.

III. Results and Discussion

A. State-to-State Rate Constants and Arrhenius Parameters. The state-to-state rate constants are given in Table I and their associated Arrhenius parameters are given in Table II. The extent to which particular state-to-state processes are classically forbidden or classically close-to-forbidden can be seen by consulting the plots of trajectory results in ref 1. The trajectory calculations of state-to-state rate constants are generally more accurate at higher temperatures than low ones, but (perhaps surprisingly) they do not seem to be more accurate in general for $n_1 = 2$ than for $n_1 = 0$. The Bessel uniform approximation of classical S matrix theory with only real-valued trajectories (BUSCCA) is more accurate than the quasiclassical trajectory histogram method for three state-to-state transitions ($1 \rightarrow 3$, $1 \rightarrow 4$, and $2 \rightarrow 4$) at all temperatures studied (300–1000 K) and for three more state-to-state transitions over part of the temperature range ($1 \rightarrow 6$ and $2 \rightarrow 6$ at low T and $2 \rightarrow 3$ at high T). For the latter three transitions at other temperatures and for the remaining nine state-to-state transitions at all temperatures, the QCTH method is more accurate. Quasiclassical trajectory reverse histogram (QCTRH) calculations are available only for the two most favorable transitions for $n_1 = 0$. For the $0 \rightarrow 3$ case, the QCTH and BUSCCA methods are both more accurate than the QCTRH method; for the $0 \rightarrow 4$ case, the QCTRH method is most accurate at low T, the QCTH method is most accurate at high T, and both are more accurate than the BUSCCA method at all T.

Thus of the three methods the QCTH method seems to give the most accurate rate constants overall. This is fortunate computationally since it is the easiest and most economical of the three methods. Even at 1000 K, however, this method yields state-to-state rate constants accurate within 20% only for 8 ($0 \rightarrow 3$, $0 \rightarrow 4$, $0 \rightarrow 5$, $0 \rightarrow 6$, $1 \rightarrow 5$, $1 \rightarrow 6$, $2 \rightarrow 4$, and $2 \rightarrow 6$) of the 15 transitions for which it yields nonzero results.

The state-to-state Arrhenius parameters are given here at only one temperature, $T = 461.54$ K. This temperature would be at the center of an Arrhenius plot ($\ln k$ vs. $1/T$) for the temperature range 300–1000 K; thus the Arrhenius energy of activation computed by the Tolman method for this temperature is about the same as would be obtained by a least-squares fit to rates at temperatures evenly spaced in $1/T$ over this temperature range. All state-to-state activation energies are accurate within 1.3 kcal/mol for the QCTH method and within 2.8 kcal/mol by the BUSCCA method. The average absolute value of the deviation is much smaller for each method, 0.4 kcal/mol for 15 transitions for the QCTH method and 0.7 kcal/mol for 14 transitions for the BUSCCA method. The BUSCCA method overestimates the activation energy in all cases and the QCTH method does so in 12 of 15 cases; this is attributable primarily to a systematic overestimation of the threshold energies by these methods.

B. State-Selected Rate Constants and Arrhenius Parameters. The state-selected rate constants are given in Table III, and their associated Arrhenius parameters are given at three temperatures in Table IV. The qualitative comparisons are similar to those for the state-to-state rate constants but the accuracy of the trajectory methods is better for these summed quantities. Again the QCTH method is more accurate than the BUSCCA method. The QCTH method predicts all three state-selected rates with an accuracy of 8% or better for $T \geq 600$ K; the largest and average errors in its predicted activation energies at $T = 461.54$ K are 0.2 and 0.1 kcal/mol, respectively. In addition, it predicts the temperature variations of the activation energies quite accurately.

TABLE I: State-to-State Rate Constants $k_{n_1 n_2}(T)$

		$k_{n_1 n_2}(T)$, cm molecule^{-1} s^{-1}			
n_1,n_2	T, K	quantum	QCTH[a]	BUSCCA[b]	QCTRH[c]
0,2	300	6.56 ± 0.21(1)[d]	1.55 ± 0.25(1)	0.00	
	400	1.80 ± 0.05(2)	6.05 ± 0.88(1)	0.00	
	600	5.25 ± 0.08(2)	2.30 ± 0.30(2)	0.00	
	1000	1.32 ± 0.01(3)	6.22 ± 0.80(2)	0.00	
0,3	300	5.86 ± 0.20(2)	4.78 ± 0.11(2)	3.75 ± 0.03(2)	8.25 ± 0.35(2)
	400	1.61 ± 0.03(3)	1.44 ± 0.02(3)	1.19 ± 0.01(3)	2.15 ± 0.10(3)
	600	4.74 ± 0.07(3)	4.63 ± 0.04(3)	3.97 ± 0.04(3)	6.06 ± 0.20(3)
	1000	1.19 ± 0.01(4)	1.27 ± 0.01(4)	1.06 ± 0.02(4)	1.50 ± 0.04(4)
0,4	300	7.46 ± 0.18(2)	6.85 ± 0.15(2)	4.73 ± 0.26(2)	7.56 ± 0.70(2)
	400	2.16 ± 0.04(3)	2.12 ± 0.06(3)	1.58 ± 0.07(3)	2.14 ± 0.14(3)
	600	6.74 ± 0.07(3)	6.70 ± 0.15(3)	5.56 ± 0.18(3)	6.41 ± 0.27(3)
	1000	1.81 ± 0.01(4)	1.73 ± 0.03(4)	1.60 ± 0.04(4)	1.62 ± 0.05(4)
0,5	300	2.97 ± 0.04(1)	8.00 ± 0.90(0)	6.71 ± 1.34(−1)	
	400	1.22 ± 0.01(2)	6.35 ± 0.54(1)	9.89 ± 1.51(0)	
	600	6.23 ± 0.03(2)	5.45 ± 0.34(2)	1.56 ± 0.17(2)	
	1000	3.02 ± 0.04(3)	3.27 ± 0.16(3)	1.50 ± 0.13(3)	
0,6	300	1.23 ± 0.11(−1)	4.86 ± 0.50(−2)	1.35 ± 0.15(−2)	
	400	1.93 ± 0.11(0)	1.27 ± 0.09(0)	5.68 ± 0.86(−1)	
	600	3.75 ± 0.14(1)	3.53 ± 0.17(1)	2.67 ± 0.53(1)	
	1000	5.05 ± 0.23(2)	5.45 ± 0.24(2)	6.08 ± 1.37(2)	
1,2	300	1.81 ± 0.07(2)	2.32 ± 0.08(2)	2.74 ± 0.52(1)	
	400	4.67 ± 0.11(2)	6.51 ± 0.17(2)	1.04 ± 0.20(2)	
	600	1.32 ± 0.02(3)	1.98 ± 0.02(3)	4.05 ± 0.80(2)	
	1000	3.32 ± 0.05(3)	5.31 ± 0.17(3)	1.17 ± 0.25(3)	
1,3	300	4.64 ± 0.17(2)	2.01 ± 0.09(2)	3.08 ± 0.23(2)	
	400	1.24 ± 0.02(3)	5.94 ± 0.20(2)	9.46 ± 0.50(2)	
	600	3.70 ± 0.04(3)	1.95 ± 0.04(3)	3.18 ± 0.12(3)	
	1000	9.93 ± 0.08(3)	5.73 ± 0.09(3)	9.20 ± 0.41(3)	
1,4	300	1.58 ± 0.10(2)	2.77 ± 0.18(2)	7.10 ± 0.61(1)	
	400	3.88 ± 0.15(2)	8.29 ± 0.44(2)	2.46 ± 0.22(2)	
	600	1.07 ± 0.02(3)	2.64 ± 0.11(3)	9.12 ± 0.70(2)	
	1000	3.05 ± 0.06(3)	7.20 ± 0.25(3)	2.98 ± 0.17(3)	
1,5	300	9.67 ± 0.17(2)	7.18 ± 0.51(2)	5.74 ± 0.72(2)	
	400	2.65 ± 0.04(3)	2.06 ± 0.12(3)	1.77 ± 0.18(3)	
	600	7.54 ± 0.09(3)	6.00 ± 0.28(3)	5.55 ± 0.42(3)	
	1000	1.76 ± 0.02(4)	1.41 ± 0.05(4)	1.39 ± 0.08(4)	
1,6	300	6.92 ± 0.93(0)	1.32 ± 0.16(1)	2.93 ± 0.43(0)	
	400	5.24 ± 0.57(1)	8.37 ± 0.77(1)	2.80 ± 0.32(1)	
	600	4.21 ± 0.35(2)	5.54 ± 0.35(2)	2.82 ± 0.24(2)	
	1000	2.33 ± 0.15(3)	2.63 ± 0.10(3)	1.87 ± 0.12(3)	
2,2	300	3.03 ± 0.07(2)	2.43 ± 0.10(2)	1.38 ± 0.12(2)	
	400	7.54 ± 0.17(2)	6.61 ± 0.22(2)	4.11 ± 0.30(2)	
	600	2.02 ± 0.05(3)	2.00 ± 0.06(3)	1.32 ± 0.09(3)	
	1000	4.87 ± 0.23(3)	5.46 ± 0.25(3)	3.49 ± 0.31(3)	
2,3	300	1.92 ± 0.03(2)	1.87 ± 0.04(2)	1.34 ± 0.14(2)	
	400	5.16 ± 0.06(2)	5.03 ± 0.09(2)	4.10 ± 0.30(2)	
	600	1.65 ± 0.02(3)	1.53 ± 0.02(3)	1.45 ± 0.07(3)	
	1000	5.17 ± 0.17(3)	4.41 ± 0.11(3)	4.74 ± 0.18(3)	
2,4	300	3.84 ± 0.08(2)	2.08 ± 0.13(2)	2.31 ± 0.16(2)	
	400	9.97 ± 0.21(2)	6.03 ± 0.34(2)	7.00 ± 0.42(2)	
	600	2.72 ± 0.06(3)	1.91 ± 0.09(3)	2.24 ± 0.12(3)	
	1000	6.36 ± 0.16(3)	5.24 ± 0.17(3)	5.93 ± 0.28(3)	
2,5	300	3.64 ± 0.09(2)	4.06 ± 0.36(2)	9.07 ± 1.04(1)	
	400	8.59 ± 0.20(2)	1.13 ± 0.08(3)	3.04 ± 0.30(2)	
	600	2.24 ± 0.03(3)	3.30 ± 0.18(3)	1.12 ± 0.09(3)	
	1000	5.55 ± 0.06(3)	8.05 ± 0.30(3)	3.54 ± 0.20(3)	
2,6	300	3.77 ± 0.65(2)	6.88 ± 0.73(2)	1.38 ± 0.33(2)	
	400	1.23 ± 0.18(3)	1.82 ± 0.17(3)	5.34 ± 1.05(2)	
	600	4.00 ± 0.48(3)	4.83 ± 0.36(3)	2.07 ± 0.32(3)	
	1000	1.01 ± 0.10(4)	1.06 ± 0.06(4)	6.06 ± 0.70(3)	

[a] Quasiclassical trajectory histogram method. [b] Bessel uniform semiclassical method with only real-valued trajectories. [c] Quasiclassical trajectory reverse histogram method, ref 1. [d] This means (6.56 ± 0.21) × 10^1.

C. State-Selected Fractions of Final Energy in Vibration. Figure 1 shows the computed fractions $f_{n_1}(E)$ of available excitation energy released as vibrational excitation energy of the product as a function of energy. This figure shows that the fraction of energy predicted to be in vibration by the quasiclassical trajectory histogram (QCTH) method and the Bessel uniform semiclassical approximation of classical S matrix theory with only real-valued trajectories (BUSCCA) is in reasonable agreement with the quantum results (notice that the

TABLE II: Arrhenius Parameters for State-to-State Rate Constants at $T = 461.54$ K[a]

	quantum		QCTH		BUSCCA	
n_1,n_2	$A(n_1,n_2,T)$	$E_a(n_1,n_2,T)$	$A(n_1,n_2,T)$	$E_a(n_1,n_2,T)$	$A(n_1,n_2,T)$	$E_a(n_1,n_2,T)$
0,2	4.35(3)[b]	2.54	3.39(3)	3.20		
0,3	3.98(4)	2.55	4.62(4)	2.76	4.31(4)	2.85
0,4	6.33(4)	2.69	6.64(4)	2.74	6.68(4)	2.98
0,5	1.43(4)	3.80	3.87(4)	5.10	3.77(4)	6.56
0,6	1.27(4)	7.00	2.64(4)	7.91	5.69(4)	9.16
1,2	1.01(4)	2.45	1.76(4)	2.63	6.11(3)	3.24
1,3	3.11(4)	2.57	1.98(4)	2.80	3.44(4)	2.86
1,4	7.61(3)	2.38	2.60(4)	2.74	1.19(4)	3.09
1,5	6.03(4)	2.49	5.05(4)	2.54	5.44(4)	2.73
1,6	2.66(4)	4.96	2.37(4)	4.49	2.79(4)	5.49
2,2	1.40(4)	2.33	1.71(4)	2.60	1.32(4)	2.76
2,3	1.54(4)	2.71	1.32(4)	2.60	1.67(4)	2.96
2,4	1.99(4)	2.38	1.84(4)	2.72	2.23(4)	2.76
2,5	1.44(4)	2.25	2.76(4)	2.54	1.44(4)	3.07
2,6	4.25(4)	2.82	3.40(4)	2.33	3.14(4)	3.24

[a] $A(n_1,n_2,T)$ and $E_a(n_1,n_2,T)$ have units of cm molecule^{-1} s^{-1} and kcal mol^{-1}, respectively. [b] This means 4.35×10^3.

TABLE III: State-Selected Rate Constants

		$k_{n_1}(T)$, cm molecule^{-1} s^{-1}		
n_1	T, K	quantum	QCT[a]	BUSCCA
0	300	1.41 ± 0.02(3)[b]	1.19 ± 0.02(3)	8.43 ± 0.12(2)
	400	4.06 ± 0.05(3)	3.69 ± 0.05(3)	2.77 ± 0.03(3)
	600	1.27 ± 0.01(4)	1.22 ± 0.01(4)	9.67 ± 0.08(3)
	1000	3.50 ± 0.02(4)	3.46 ± 0.02(4)	2.84 ± 0.02(4)
1	300	1.83 ± 0.05(3)	1.44 ± 0.04(3)	1.02 ± 0.12(3)
	400	4.90 ± 0.08(3)	4.22 ± 0.09(3)	3.18 ± 0.29(3)
	600	1.42 ± 0.01(4)	1.31 ± 0.02(4)	1.06 ± 0.06(4)
	1000	3.66 ± 0.02(4)	3.52 ± 0.03(4)	2.98 ± 0.11(4)
2	300	1.65 ± 0.03(3)	1.72 ± 0.03(3)	6.69 ± 0.39(2)
	400	4.42 ± 0.09(3)	4.71 ± 0.07(3)	2.20 ± 0.10(3)
	600	1.28 ± 0.02(4)	1.36 ± 0.01(4)	7.80 ± 0.24(3)
	1000	3.27 ± 0.03(4)	3.44 ± 0.02(4)	2.31 ± 0.04(4)

[a] When the histogram aspect of the QCTH method is not involved it may be called simply the quasiclassical trajectory (QCT) method. [b] This means $(1.41 \pm 0.02) \times 10^3$.

TABLE IV: Arrhenius Parameters for State-Selected Rate Constants[a]

		quantum		QCT		BUSCCA	
n_1	T, K	$A(n_1,T)$	$E_a(n_1,T)$	$A(n_1,T)$	$E_a(n_1,T)$	$A(n_1,T)$	$E_a(n_1,T)$
0	300.00	8.56(4)[b]	2.45	1.02(5)	2.65	9.10(4)	2.79
	461.54	1.18(5)	2.68	1.28(5)	2.82	1.14(5)	2.96
	1000.00	1.79(5)	3.24	1.83(5)	3.31	1.55(5)	3.37
1	300.00	8.30(4)	2.27	9.72(4)	2.51	8.75(4)	2.65
	461.54	1.15(5)	2.51	1.23(5)	2.68	1.13(5)	2.84
	1000.00	1.66(5)	3.00	1.67(5)	3.10	1.52(5)	3.23
2	300.00	7.30(4)	2.26	8.93(4)	2.35	6.74(4)	2.75
	461.54	1.04(5)	2.51	1.10(5)	2.51	9.51(4)	3.00
	1000.00	1.45(5)	2.96	1.49(5)	2.92	1.25(5)	3.35

[a] $A(n_1,T)$ and $E_a(n_1,T)$ have units of cm molecule^{-1} s^{-1} and kcal mol^{-1}, respectively. [b] This means 8.56×10^4.

ordinate scale is expanded, i.e, the total range shown is 0.4–0.8, not 0–1). The results of averaging these predictions over Maxwell–Boltzmann translational distributions are shown in Table V. For $n_1 = 0$ and 1, the agreement of trajectory and quantal calculations is excellent. For $n_1 = 2$ the agreement is good at higher temperature, but the QCTH method overestimates the vibrational excitation by a factor of 1.1 at room temperature.

D. Thermally Averaged Rate Constants for Production of Specific Vibrational States and Fraction of Final Energy in Vibration. Table VI gives the results of averaging the state-to-state rate constants over a Boltzmann distribution of initial vibrational states and Table VII gives the mean final fraction of energy in vibration as computed from Table VI and from the results for $n_2 = 0$–1. Table VII may also be considered to be the result of averaging Table V over initial vibrational states. The results in these two tables are of special interest because of the widespread use of trajectory calculations for interpreting and predicting final state distributions of chemical reactions.[22] Table VII shows that the first moment of the final vibrational distribution is predicted quite accurately by both methods at all temperatures. Table VI shows that the complete distribution as a function of n_2 is predicted more accurately by the QCTH method than the BUSCCA method. Further, it is predicted quite reliably by the QCTH method at 1000 K. Although the QCTH method gives an accurate first moment at 300 K, the actual distribution is not accurate at that temperature.

E. Thermal Rate Constants and Arrhenius Parameters. The thermal rate constants are given in Table VIII and the associated Arrhenius parameters are in Table IX. At

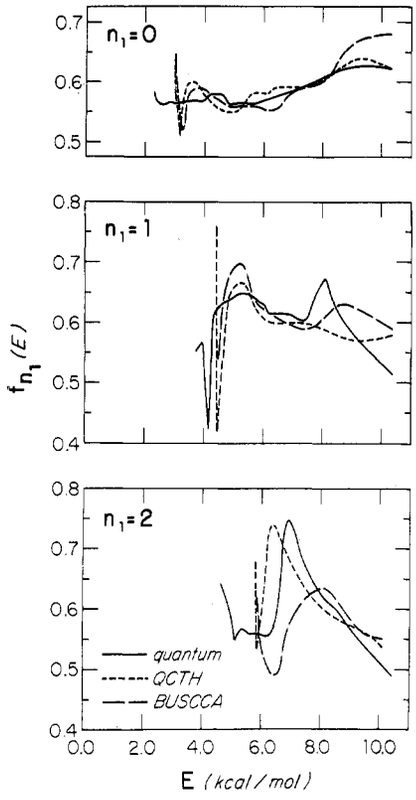

Figure 1. Fraction $f_{n_1}(T)$ of available excitation energy which is released as vibrational excitation energy of the product HCl as a function of total energy for the quantum mechanical (—), quasiclassical trajectory histogram (-----), and Bessel uniform semiclassical (— —) calculations.

TABLE V: The Fraction $f_{n_1}(T)$ of Available Excitation Energy in Product Vibrational Excitation for Reactants with Initial Vibrational Quantum Numbers n_1 at Translation Temperature T

		$f_{n_1}(T)$		
n_1	T, K	quantum	QCTH[a]	BUSCCA[a]
0	300	0.58	0.58	0.58
	400	0.58	0.58	0.58
	600	0.58	0.58	0.58
	1000	0.57	0.58	0.58
1	300	0.64	0.65	0.67
	400	0.65	0.65	0.67
	600	0.65	0.65	0.66
	1000	0.64	0.63	0.65
2	300	0.66	0.73	0.63
	400	0.67	0.73	0.64
	600	0.67	0.71	0.65
	1000	0.65	0.68	0.64

[a] Reference 1.

temperatures up to 600 K less than 2% of the thermal rate comes from states with $n_1 > 2$, but our estimates of these higher-state rate constants contribute about 10% of the rate at 1000 K. Including these estimates the QCTH rate constants are accurate within 16, 9, 4, and 1% at 300, 400, 600, and 1000 K, respectively. The BUSCCA rates are significantly lower due to serious systematic overestimation of threshold energies. This also makes the BUSCCA activation energy at T = 461.54 K too high by 0.26 kcal/mol, whereas the QCTH one is accurate within 0.14 kcal/mol.

It is also interesting to compare the trajectory results to transition-state theory.[1,23] This is done in Table VIII. At 300–600 K, the QCTH calculations are in remarkable agreement with conventional transition-state theory

TABLE VI: Rate Constants for Production of Specific Final States

		$k^{n_2}(T)$, cm molecule^{-1} s^{-1}		
n_2	T, K	quantum	QCTH	BUSCCA
2	300	7.44(1)[a]	3.10(1)	2.50(0)
	400	2.23(2)	1.41(2)	1.94(1)
	600	7.50(2)	6.62(2)	1.50(2)
	1000	2.08(3)	2.26(3)	6.80(2)
3	300	5.75(2)	4.58(2)	3.69(2)
	400	1.54(3)	1.32(3)	1.15(3)
	600	4.27(3)	3.84(3)	3.60(3)
	1000	9.46(3)	8.79(3)	8.56(3)
4	300	7.05(2)	6.55(2)	4.45(2)
	400	1.92(3)	1.93(3)	1.41(3)
	600	5.28(3)	5.52(3)	4.36(3)
	1000	1.13(4)	1.18(4)	1.01(4)
5	300	9.36(1)	5.71(1)	3.92(1)
	400	4.35(2)	3.20(2)	2.24(2)
	600	2.05(3)	1.75(3)	1.26(3)
	1000	6.59(3)	6.15(3)	4.63(3)
6	300	2.43(0)	4.32(0)	8.88(−1)
	400	2.87(1)	4.19(1)	1.29(1)
	600	3.23(2)	3.91(2)	1.85(2)
	1000	1.98(3)	2.14(3)	1.47(3)

[a] This means 7.44 × 10¹.

TABLE VII: Average Fraction $f(T)$ of Available Excitation Energy in Product Vibrational Excitation in a Thermal System at Temperature T

	$f(T)$		
T, K	quantum	QCTH[a]	BUSCCA[a]
300	0.59	0.59	0.58
400	0.59	0.59	0.59
600	0.60	0.60	0.60
1000	0.61	0.61	0.61

[a] Reference 1.

calculations with transmission coefficient unity (TST). At 1000 K, however, transition state theory overestimates the quantal rate by 5% presumably due to classical recrossing effects, which have been studied elsewhere.[24] The success of transition-state theory in accounting for the quantal rates reported here is encouraging because transition-state theory calculations are much easier and less time consuming to carry out. Including the simple Wigner correction factor[25]

$$\kappa(T) = 1 + (h|\omega^{\ddagger}|/kT)^2/24 \qquad (26)$$

(where $\omega^{\ddagger}$ is the imaginary frequency of the reaction coordinate normal mode) in transition state theory to account approximately for the quantum mechanical character of reaction-coordinate motion improves the agreement with the quantal results to 3% over the 300–600-K temperature range.

IV. Summary

The quasiclassical trajectory method has been shown to yield a rate constant accurate within 16% over the 300–1000-K temperature range for the collinear H + Cl_2 reaction. The temperature-dependent energy of activation is only 0.1–0.2 kcal/mol too high over this range. The final vibrational state distribution is accurate at 1000 K but not 300 K, although the average final vibrational energy is accurate within 1% over the whole temperature range. State-selected and state-to-state rate constants show larger deviations from the quantal results. The Bessel uniform approximation of classical S matrix theory using only

TABLE VIII: Thermal Rate Constants

T, K	quantum	QCT	BUSCCA	TST[a]	TST/W[b]
		$k(n_1 \leq 2, T)$, cm molecule^{-1} s^{-1}			
300	1.44(3)[c,d]	1.21(3)	8.54(2)		
400	4.16(3)[d]	3.76(3)	2.80(3)		
600	1.27(4)[d]	1.22(4)	9.54(3)		
1000	3.17(4)	3.13(4)	2.53(4)		
		$k(T)$, cm molecule^{-1} s^{-1}			
300	1.44(3)	1.21(3)	8.54(2)	1.21(3)	1.49(3)
400	4.17(3)	3.78(3)	2.81(3)	3.81(3)	4.29(3)
600	1.30(4)	1.25(4)	9.71(3)	1.27(4)	1.34(4)
1000	3.49(4)	3.47(4)	2.76(4)	3.68(4)	3.75(4)

[a] Conventional transition state theory, ref 1 and 23. [b] Transition state theory with Wigner tunneling correction, ref 23. [c] This means 1.44×10^3. [d] These results agree with those in ref 2 within 2%.

TABLE IX: Arrhenius Parameters for Thermal Rate Constants $k(T)$ and Quantities in Eq 15-19[a]

T, K	$\langle E_{rel} \rangle^T_{reactions}$	$\langle E_n^v \rangle^T_{reactions}$	$^1/_2 kT$	$\langle E_{n_1}^v \rangle^T$	$E_a^{rel}(T)$	$E_a^v(T)$	$E_a(T)$	$A(T)$
				Quantum Mechanics				
200.00	2.44	0.84	0.20	0.82	2.24	0.02	2.25	5.80(4)[b]
250.00	2.59	0.89	0.25	0.86	2.34	0.02	2.37	7.53(4)
300.00	2.73	0.95	0.30	0.92	2.43	0.03	2.46	8.94(4)
400.00	2.97	1.09	0.40	1.05	2.57	0.04	2.60	1.10(5)
461.54	3.10	1.18	0.46	1.14	2.64	0.04	2.67	1.20(5)
600.00	3.35	1.40	0.60	1.38	2.76	0.02	2.78	1.34(5)
1000.00	3.93	2.09	0.99	2.13	2.94	−0.04	2.90	1.50(5)
				QCT				
200.00	2.74	0.84	0.20	0.82	2.54	0.01	2.55	8.32(4)
250.00	2.84	0.88	0.25	0.86	2.59	0.02	2.61	9.54(4)
300.00	2.94	0.94	0.30	0.92	2.64	0.03	2.67	1.06(5)
400.00	3.12	1.09	0.40	1.05	2.73	0.04	2.76	1.22(5)
461.54	3.23	1.19	0.46	1.14	2.77	0.04	2.81	1.30(5)
600.00	3.45	1.42	0.60	1.38	2.86	0.04	2.90	1.42(5)
1000.00	3.98	2.12	0.99	2.13	2.99	−0.04	2.98	1.56(5)
				Semiclassical (BUSCCA)				
200.00	2.87	0.84	0.20	0.82	2.67	0.01	2.68	7.30(4)
250.00	2.97	0.88	0.25	0.86	2.73	0.02	2.74	8.41(4)
300.00	3.08	0.93	0.30	0.92	2.78	0.02	2.80	9.29(4)
400.00	3.27	1.06	0.40	1.05	2.87	0.01	2.88	1.06(5)
461.54	3.38	1.14	0.46	1.14	2.93	0.01	2.93	1.11(5)
600.00	3.62	1.35	0.60	1.38	3.02	−0.03	3.00	1.20(5)
1000.00	4.13	2.00	0.99	2.13	3.13	−0.13	3.01	1.25(5)

[a] $A(T)$ and $E_a(T)$ have units of cm molecules^{-1} s^{-1} and kcal mol^{-1}, respectively. [b] This means 5.80×10^4.

real-valued trajectories is less accurate than the quasiclassical trajectory histogram method, and running the trajectories backward does not improve the results either. Although the degree of agreement between quantum mechanical and trajectory results depends upon the specific system studied, we hope the results for the present system will provide a useful guideline for the general extent of agreement which can be expected in other similar cases.

Acknowledgment. This work was supported in part by the National Science Foundation under Grant No. CHE77-27415.

Supplementary Material Available: A list of the quantum mechanical state-to-state reaction probabilities and state-selected reaction probabilities is given in Table A-1 (3 pages). Ordering information is available on any current masthead page.

References and Notes

(1) D. G. Truhlar, J. A. Merrick, and J. W. Duff, *J. Am. Chem. Soc.*, **98**, 6771 (1976). Errata: On p 6771, column 2, line 13, it should read: only for H + H_2, Cl + H_2, F + H_2, and some of their isotopic analogues.[14b,15,18,19] The first few entries of the last column of Table IV are in error; see Table VIII of present article. In Table A-7, row 3, 3.83 should be 8.83.
(2) H. Essen, G. D. Billing, and M. Baer, *Chem. Phys. Lett.*, **17**, 443 (1976).
(3) M. Karplus, R. N. Porter, and R. D. Sharma, *J. Chem. Phys.*, **43**, 3259 (1965).
(4) L. M. Raff and M. Karplus, *J. Chem. Phys.*, **44**, 1212 (1966).
(5) K. G. Anlauf, J. C. Polanyi, W. H. Wong, and K. B. Woodall, *J. Chem. Phys.*, **49**, 5189 (1968).
(6) J. M. Bowman and A. Kuppermann, *J. Chem. Phys.*, **59**, 6254 (1973).
(7) J. M. Bowman, G. C. Schatz, and A. Kuppermann, *Chem. Phys. Lett.*, **24**, 378 (1974).
(8) J. R. Stine and R. A. Marcus, *J. Chem. Phys.*, **59**, 5145 (1973).
(9) W. H. Miller, *Adv. Chem. Phys.*, **30**, 77 (1975).
(10) J. W. Duff and D. G. Truhlar, *Chem. Phys. Lett.*, **40**, 251 (1976).
(11) M. Baer, *J. Chem. Phys.*, **60**, 1057 (1974); M. Baer, unpublished results. In ref 1 we used the former results for initial vibrational quantum number $n_1 = 0$ and 1 and the latter results for $n_1 = 2$.
(12) D. G. Truhlar and J. C. Gray, *Chem. Phys. Lett.*, **57**, 93 (1978). In this communication the sums over n_1 were not all converged; the only qualitatively important change is for H_2 + I at $T > 1500$ K for which a more careful calculation eliminates the maximum in $E_a(T)$. Table IX of the present article supersedes Table 1 of the communication.
(13) D. G. Truhlar and A. Kuppermann, *J. Chem. Phys.*, **56**, 2232 (1972); J. M. Bowman and A. Kuppermann, *Chem. Phys. Lett.*, **12**, 1 (1972).
(14) G. C. Schatz, J. M. Bowman, and A. Kuppermann, *J. Chem. Phys.*, **63**, 674 (1975).
(15) G. C. Schatz, J. M. Bowman, and A. Kuppermann, *J. Chem. Phys.*, **63**, 685 (1975).
(16) J. C. Gray, D. G. Truhlar, L. Clemens, J. W. Duff, F. M. Chapman, Jr., G. O. Morrell, and E. F. Hayes, *J. Chem. Phys.*, **69**, 240 (1978).
(17) G. C. Schatz and A. Kuppermann, *J. Chem. Phys.*, **65**, 4668 (1976).
(18) M. Baer, U. Halavee, and A. Persky, *J. Chem. Phys.*, **61**, 5122 (1974).
(19) D. G. Truhlar, *J. Phys. Chem.*, **83**, 188 (1979).
(20) P. J. Kuntz, E. M. Nemeth, J. C. Polanyi, S. D. Rosner, and C. E. Young, *J. Chem. Phys.*, **44**, 1168 (1966).
(21) D. G. Truhlar, *J. Chem. Educ.*, **55**, 309 (1978). The bracketed

denominator in eq 34 should be squared.

(22) See, for example, ref 4, 5, and 20; R. L. Wilkins in "Handbook of Chemical Lasers", R. W. F. Gross and J. F. Bott, Ed., Wiley-Interscience, New York, 1976, p 551; D. G. Truhlar and D. A. Dixon in "Atom-Molecule Collision Theory: A Guide for the Experimentalist", R. B. Bernstein, Ed., Plenum Press, New York, 1979, in press.

(23) B. C. Garrett and D. G. Truhlar, unpublished results. The transition-state parameters are $r^{\ddagger}_{HCl} = 4.254\ a_0$, $r^{\ddagger}_{ClCl} = 3.811\ a_0$, $V^{\ddagger} = 2.420$ kcal/mol, $\hbar\omega_e^{str} = 1.478$ kcal/mol = 523.9 cm^{-1}, $x_e^{str} = 6.731 \times 10^{-3}$, $\hbar\omega^{\ddagger} = 1.395i$ kcal/mol = 487.9i cm^{-1}. The reactant parameters are $r_e^{ClCl} = 3.779\ a_0$, $\hbar\omega_e^{ClCl} = 1.606$ kcal/mol = 561.9 cm^{-1}, $x_e^{ClCl} = 6.919 \times 10^{-3}$.

(24) B. C. Garrett and D. G. Truhlar, *J. Phys. Chem.*, following paper in this issue.

(25) E. P. Wigner, *Z. Phys. Chem. B*, **19**, 203 (1932); H. S. Johnston, "Gas-Phase Reaction Rate Theory", Ronald Press, New York, 1966, pp 133–136; D. Rapp, "Statistical Mechanics", Holt, Rinehart and Winston, New York, 1966, pp 133–136.

Generalized Transition State Theory. Classical Mechanical Theory and Applications to Collinear Reactions of Hydrogen Molecules

Bruce C. Garrett and Donald G. Truhlar*

Chemical Dynamics Laboratory, Kolthoff and Smith Halls, Department of Chemistry, University of Minnesota, Minneapolis, Minnesota 55455 *(Received August 9, 1978)*

We consider classical versions of three generalizations of transition state theory: microcanonical variational transition state theory, canonical variational transition state theory, and Miller's unified statistical theory. We prove that microcanonical variational transition state theory is identical with the adiabatic theory of reactions, i.e., to adiabatic transition state theory. To test the validity of these approximate theories, we present calculations for several collinear reactions of hydrogen and halogen atoms with hydrogen molecules. Average reaction probabilities are computed using conventional and microcanonical variational transition state theory and the unified statistical theory and are compared with those of exact classical dynamics for seven cases. These results confirm the general validity of the fundamental assumption of transition state theory at low energy and show that the variational method can be used to extend the range of validity to higher energies. Thermal rate constants are calculated by these methods and by canonical variational transition state theory for nine systems. Using a Morse approximation involving the second and third derivatives of the local vibrational well at its minimum, the average absolute value of the error and range of absolute values of the errors at 600 K for the seven cases where we computed exact classical canonical rate constants are 28 and 0–78% for conventional transition state theory, 10 and 1–37% for the microcanonical variational theory or adiabatic transition state theory, 7 and 1–22% for the unified statistical theory, and 15 and 0–41% for the canonical variational theory.

I. Introduction

Recent attempts to develop a useful quantum mechanical version of transition state theory have led to a more careful examination of the dynamical foundation of transition state theory.[1] The fundamental dynamical assumption may be expressed unequivocally only in classical mechanics, where it may be stated as follows: Transition state theory with unit transmission coefficient is exact if and only if all trajectories through the transition state, which is a surface dividing reactants from products, cross this surface only once.[2-5] Further if trajectories do recross this surface, transition state theory with unit transmission coefficient overestimates the rate. Transition state theory may also be derived on the basis of a quasi-equilibrium postulate; this is the traditional basis of the theory,[6-10] but it does not lead to the same kind of interpretation as the dynamical justification. One approach to reconciling the quasi-equilibrium assumption with a dynamical model is the adiabatic theory of reactions; the adiabatic theory assumes that all the degrees of freedom which remain bound throughout the course of the reaction adjust adiabatically to progress of the system along a separable reaction coordinate.[10-20] It is now realized that the adiabatic assumption and the quasi-equilibrium assumption do not lead to identical results,[20] but the adiabatic assumption still provides a useful framework in which to include quantum mechanical effects on motion along a reaction coordinate which is assumed separable.[10,21-24] Another advantage of the adiabatic theory is that one can easily include total angular momentum conservation.[13,17,25-27] The adiabatic theory of reactions is also called adiabatic transition state theory;[28] with additional assumptions about product states it is called the statistical adiabatic channel model.[25-27]

The dynamical justification of transition state theory in terms of classical trajectories not recrossing a dividing surface leads to the classical variational versions of transition state theory.[1,4,13,29-34] In these versions, the position of the dividing surface is varied so that the calculated rate is minimized. The adiabatic theory of reactions and variational transition state theory lead to generalizations of the conventional transition state which may usefully be labeled generalized transition states.[35,36]

The adiabatic theory of reactions is not really transition state theory. Although the generalized transition states of the variational transition state theories are still dividing surfaces in phase space between reactants and products, in the adiabatic theory they are not.[37] Nevertheless we show in this article that adiabatic transition state theory leads to the same rate constants, at least classically, as one version of variational transition state theory.

The dynamical justification of transition state theory with unit transmission coefficient in terms of the recrossing criterion is expected to be most valid at low energy.[3,4,38-40]

0022-3654/79/2083-1052$01.00/0